Numerical Study of the Skin Friction on a Spheroid at Incidence

M. Rosenfeld,* M. Israeli,† and M. Wolfshtein‡
Technion, Israel Institute of Technology, Haifa, Israel

This paper is concerned with a numerical solution of the three-dimensional, incompressible, steady laminar flowfield about a prolate spheroid at incidence. The governing equations were simplified by neglecting the streamwise diffusion terms to yield the so-called parabolized Navier-Stokes equations. The number of equations and the number of dependent variables are identical to those of the full Navier Stokes equations (although the mathematical character of the equations becomes simpler). Therefore, the equations are valid in separated regions whereas the parabolic boundary-layer equations are not. The three-dimensional case was solved using a curvilinear orthogonal coordinate system and primitive variables. An efficient numerical method particularly suitable to the parabolized Navier-Stokes equations was used. The paper concentrates on the distribution of the skin-friction lines for two test cases. In the first test case, the axes ratio of the spheroid was 4:1, with incidence of 6 deg and a Reynolds number (based on half the major axis) of 10^6. In the second case the axes ratio was 6:1, with incidence of 10 deg and a Reynolds number of $0.8.10^6$. Favorable agreement with experimental results was obtained in the laminar regions. Some properties of the flowfield near the body are discussed on the basis of the pattern of the skin-friction lines and the shape of the separation lines. Yet no definite conclusions on the flow pattern in the separated region can be drawn from the skin-friction results alone.

Introduction

THE analysis of incompressible three-dimensional flows around slender bodies at incidence is very important in modern aerodynamics and hydrodynamics. The flowfield is characterized by crossflow reversal, local thickening of the boundary layer, formation of longitudinal vortices, regions of backward flow, and strong viscous-inviscid interaction.[1] This complicated flowfield is of special importance to aerodynamic designers who are interested in aerodynamic coefficients and the stability of flight vehicles. In particular, the flow separation patterns become rather complicated. While in two-dimensional flows the point of flow separation coincides with the point at which the wall shear stress vanishes, in three-dimensional flows such a unique criterion does not exist. Indeed, the shear stress does not vanish on the separation line except at a limited number of points called critical or singular points. The phenomenon of flow separation over three-dimensional bodies is still far from being completely understood. Many of the studies rely on observations drawn from the analysis of the flow pattern near the body. Particularly fruitful results were obtained by visualization with oil streak techniques[2] of the limiting streamlines, the projection of which coincides with the skin-friction lines on the surface of wind tunnel models.

Lighthill[3] showed that the number and type of singular points on a closed body must satisfy certain topological laws. These laws limit the number of possible topological patterns of the skin-friction lines and enhance the theoretical study of three-dimensional flowfields. Numerous studies[1,3-9] were conducted to find the relationship between the pattern of the skin-friction lines and the flowfield around an aerodynamic body. In particular it was often suggested that there is a correlation between the skin-friction lines and the separation phenomena that may be used to identify and classify the separation of the flow from solid bodies. It is widely accepted now that a necessary condition for flow separation in three-dimensional flowfields is the convergence of many skin-friction lines into a single line.[1] Yet it appears to be an insufficient condition[1,7,9] for separation.

A problem discussed in numerous articles[1,5,8] is the topological characteristics of separation lines. The issue is whether the separation lines must originate from a singular point and whether they are envelopes of limiting streamlines or just limiting streamlines. It is usually accepted that a separation line is a limiting streamline (skin-friction line)[1,3,8] and that in certain kinds of flow separation, the separation lines originate from one or more singular points.[1,3,7,9] Yet it has been shown[8,9] that separated vortices may start at a line that does not originate from a singular point on the body. Classification of three-dimensional flow separation according to the pattern of the singular points and of the skin-friction lines on the body was attempted in several studies.[5,8,9] However, a unique relationship between an observed flow pattern near a body and the structure of the flow does not necessarily exist, as was pointed out by Dallman.[7]

As the phenomenon considered is so complicated, much of the research on incompressible flow was restricted to simpler geometries. One such geometry is the prolate spheroid, which has been studied relatively extensively experimentally[6,10] and numerically.[11-20] In most of the numerical calculations, the boundary-layer approximation was used. For instance, Wang[11] solved the degenerate case of the boundary-layer equations at the windward and leeward symmetry planes. Later Wang[12] computed the flowfield around a spheroid of major to minor axis ratio of 4:1 at 6 deg incidence. A solution was obtained over a significant portion of the body. No solution could be found at the rear part of the spheroid because of numerical instabilities. Wang concluded that flow separation occurred there. Cebeci et al.[13]

Received March 1, 1986; revision received June 1, 1987.

*Graduate Instructor, Department of Aeronautical Engineering; presently NRC Research Associate, NASA Ames Research Center, Moffett Field, CA. Member AIAA.

†Professor, Department of Computer Sciences, Member AIAA.

‡Associate Professor, Department of Aeronautical Engineering. Member AIAA.

obtained very similar results for the same case and calculated the flow at other angles of attack as well. Hirsch and Cebeci[14] and Patel and Choi[15] solved the momentum equations by marching with an ADI method, which was expected to be more stable in circumferentially reversed flow regions than the usual boundary-layer schemes. In addition, Hirsch and Cebeci[14] also solved what they call the "Parabolic-Elliptic Boundary Layer" equations in which the pressure field is imposed but the circumferential diffusion terms are retained. No significant change in the results was reported.

Solutions of the boundary-layer equations for a 6:1 spheroid at incidence were reported by Schoenauer[16] and Patel and Baek,[17] among others. Schoenauer's code[16] is for general configurations and uses adaptive high-order methods with control on the truncation error bounds. Unfortunately, no easily comparable results are presented. Stock[18] solved the integral boundary-layer equations for a variety of cases. Reasonable agreement with experiments was obtained only for those regions of the flowfield in which the flow direction does not deviate significantly from that of the main outer flow. In all boundary-layer calculations, flowfields without flow reversal can be readily calculated. These methods may handle weak circumferential flow reversals as well, although some special numerical procedures are required. However, they cannot resolve separated flows.

In general, application of the boundary-layer approximation requires the specification of the pressure, say by a potential flow solution. In such calculations, the separation line cannot be reached, and the beginning of numerical instabilities are usually interpreted as the onset of separation. This numerical difficulty may be overcome by "inverse boundary-layer methods." Van Dalsem and Steger[19] solved the unsteady boundary-layer equations for the flow around a spheroid 6:1 at an incidence of 30 deg by specifying the wall shear instead of the pressure in separated zones. No singular behavior near the separation lines was reported. Yet the validity of the "regular" as well as the "inverse" boundary-layer method near and at flow-separated regions is still questionable.

With this background, the success of the thin-layer approximation in the calculation of compressible (usually supersonic) separated flows on slender bodies at incidence should be noted. This success is usually attributed to the fact that the pressure is not prescribed a priori. Pan and Pulliam[20] solved the compressible thin-layer equations for a spheroid with an axes ratio of 6:1, 10 deg incidence, and a Mach number of 0.029. They used a very fine grid of more than 280,000 points. The numerical performance of the compressible code was relatively inefficient for this very low Mach number.

A solution of the full three-dimensional laminar and incompressible Navier-Stokes equations was reported by Haase.[21] He solved the equations for a flow over a spheroid at low Reynolds numbers using vorticity/velocity formulation and a Cartesian coordinate system. Because the coordinates were not body-fitted, special techniques were used near the wall. The results appear to suffer from too low a resolution, and the agreement obtained with other results was poor.

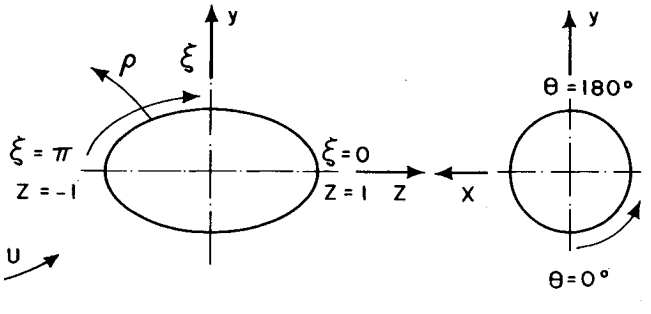

Fig. 1 The coordinate system.

In this paper, the laminar, steady, and incompressible flowfield about a prolate spheroid at incidence is investigated using numerical solutions of the parabolized Navier-Stokes equations. The equations are not singular at separation lines, and separated flow regions are included in the solution domain. Solutions of the full flowfield were obtained. Yet this paper is only concerned with a study of the pattern of the skin-friction lines. Particular attention is given to the separation lines.

Mathematical Model and Numerical Solution

The flow is approximated by the steady and incompressible Parabolized Navier-Stokes (PNS) equations obtained from the full Navier-Stokes equations by neglecting the streamwise diffusion terms in the momentum equations. These equations do not suffer from any singularity near separation because the pressure is retained as one of the dependent variables.

The governing equations are formulated in a general axisymmetric curvilinear orthogonal coordinate system using primitive variables. The three orthogonal coordinates ρ, θ, ζ (see Fig. 1) run in the normal, circumferential, and the mainstream directions, approximately. These coordinates are redistributed by one-dimensional stretching functions into another orthogonal coordinate system q, s, t, respectively. The corresponding velocity components are u, v, w, in the directions q, s, t, respectively. They are scaled by

$$u = h_q V_q \tag{1a}$$

$$v = h_s V_s \tag{1b}$$

$$w = h_t V_t \tag{1c}$$

where V_q, V_s, V_t are velocity components in the coordinates' direction. The resulting equations are the continuity equation

$$\frac{\partial(\sigma u)}{\partial q} + \frac{\partial(\tau v)}{\partial s} + \frac{\partial(\delta w)}{\partial t} = 0 \tag{2a}$$

the q-component momentum equation

$$\frac{1}{h_q} M\left(\frac{u}{h_q}\right) + \frac{1}{2}\sigma\frac{\partial\beta}{\partial q}v^2 + \frac{1}{2}\sigma\frac{\partial\gamma}{\partial q}w^2 - \frac{1}{2}\delta\frac{\partial\alpha}{\partial t}uv = -\sigma\frac{\partial p}{\partial q} + \frac{1}{Re}\left\{\frac{\partial}{\partial q}\left[\alpha\frac{\partial(\sigma u)}{\partial q}\right] + \frac{1}{\delta}\frac{\partial^2 u}{\partial s^2} + \frac{\partial}{\partial q}\left(\frac{1}{\delta}\right)\frac{\partial v}{\partial s} - \frac{\partial}{\partial q}\left(\delta\frac{\partial\alpha}{\partial t}w\right)\right\} \tag{2b}$$

the s-component momentum equation

$$\frac{1}{h_s} M\left(\frac{v}{h_s}\right) - \frac{1}{2}\delta\frac{\partial\beta}{\partial t}vw - \frac{1}{2}\sigma\frac{\partial\beta}{\partial q}uv = -\tau\frac{\partial p}{\partial s} + \frac{1}{Re}\left[\tau\beta\frac{\partial^2 v}{\partial s^2} + \frac{\partial}{\partial q}\left(\frac{1}{\delta}\frac{\partial v}{\partial q}\right) - \delta\frac{\partial\beta}{\partial t}\frac{\partial w}{\partial s} - \sigma\frac{\partial\beta}{\partial q}\frac{\partial u}{\partial s}\right] \tag{2c}$$

the t-component momentum equation

$$\frac{1}{h_t} M\left(\frac{w}{h_t}\right) + \frac{1}{2}\delta\frac{\partial\beta}{\partial t}v^2 + \frac{1}{2}\delta\frac{\partial\alpha}{\partial t}u^2 - \frac{1}{2}\sigma\frac{\partial\gamma}{\partial q}uv = -\delta\frac{\partial p}{\partial t} + \frac{1}{Re}\left\{\frac{\partial}{\partial q}\left(\frac{1}{\tau}\frac{\partial w}{\partial q}\right) + \frac{1}{\sigma}\frac{\partial^2 w}{\partial s^2} + \frac{\partial}{\partial q}\left[\frac{\partial}{\partial t}\left(\frac{1}{\tau}\right)u\right] + \frac{\partial}{\partial t}\left(\frac{1}{\sigma}\right)\frac{\partial v}{\partial s}\right\} \tag{2d}$$

$$M=\sigma u\frac{\partial}{\partial q}+\tau v\frac{\partial}{\partial s}+\delta w\frac{\partial}{\partial t} \tag{3a}$$

$$\alpha=\frac{1}{h_q^2}\qquad \sigma=\alpha J \tag{3b}$$

$$\beta=\frac{1}{h_s^2}\qquad \tau=\beta J \tag{3c}$$

$$\gamma=\frac{1}{h_t^2}\qquad \delta=\gamma J \tag{3d}$$

and J is the Jacobian:

$$J=h_q h_s h_t \tag{3e}$$

The scale factors h_q, h_s, and h_t are given by

$$h_q^2=\sum_{i=1}^{3}\left(\frac{\partial X_i}{\partial q}\right)^2 \tag{4a}$$

$$h_s^2=\sum_{i=1}^{3}\left(\frac{\partial X_i}{\partial s}\right)^2 \tag{4b}$$

$$h_t^2=\sum_{i=1}^{3}\left(\frac{\partial X_i}{\partial t}\right)^2 \tag{4c}$$

where (X_1,X_2,X_3) are the Cartesian coordinates.

In the present study, a prolate spheroidal coordinate system was chosen with the following scale factors:

$$h_q=a\frac{\mathrm{d}\rho(q)}{\mathrm{d}q}\left[\sinh^2\rho(q)+\sin^2(t)\right]^{1/2} \tag{5a}$$

$$h_s=a\frac{\mathrm{d}\theta(s)}{\mathrm{d}s}\sinh\rho(q)\,\sin\zeta(t) \tag{5b}$$

$$h_t=a\frac{\mathrm{d}\zeta(t)}{\mathrm{d}t}\left[\sinh^2\rho(q)+\sin^2\zeta(t)\right]^{1/2} \tag{5c}$$

$$a=\frac{1}{T}\sqrt{T^2-1} \tag{5d}$$

$\rho(q)$, $\theta(s)$, and $\zeta(t)$ are one-dimensional stretching functions, and T is the axes ratio.

The computed flowfield did not cover the entire prolate spheroid. The upstream boundary was placed some distance downstream of the forward stagnation point at a region where the boundary-layer approximation can still be justified and can provide the upstream boundary conditions for the PNS equations

$$u=u_{\mathrm{up}},\qquad v=v_{\mathrm{up}},\qquad w=w_{\mathrm{up}} \tag{6a}$$

where the subscript "up" stands for upstream conditions.

The downstream boundary was placed ahead of the rear stagnation point in order to minimize the usage of computational resources. It should be emphasized once again that the PNS equations are not singular at reversed-flow regions, yet the separation at the rear part, which usually has backward flow regions and strong viscous-inviscid interaction, can be accurately computed only if the downstream boundary is moved far enough into the wake. Moreover, the calculation near the rear stagnation point was found to increase the number of iterations required for the solution of the difference equations. As a result, the total demand of computer resources became too high (for the computer we used) when the region was extended to the rear of the body.

Due to parabolization, it is necessary to specify only one condition at the downstream boundary. We chose to specify a Nuemann-type boundary condition for the pressure:

$$\frac{\partial p}{\partial t}=\left(\frac{\partial p}{\partial t}\right)_{\mathrm{pot}} \tag{6b}$$

where "pot" stands for the potential value.

The outer boundary is supposed to be in the potential flow region. Three boundary conditions should be specified there. We chose the potential values of the pressure as well as the streamwise and circumferential velocity components

$$v=v_{\mathrm{pot}},\qquad w=w_{\mathrm{pot}},\qquad p=p_{\mathrm{pot}} \tag{6c}$$

The normal velocity u is not prescribed at this boundary. Therefore, the displacement near the wall due to the no-slip condition could be accounted for. On the body, the usual no-slip and no-injection conditions were used:

$$u=v=w=0 \tag{6d}$$

Because of the symmetry of the flow, the solution was obtained for half of the field only. On the leeward and windward symmetry planes, symmetry conditions were used.

The finite-difference equations written over a staggered grid were solved iteratively by marching in the streamwise direction. The procedure is consistent and stable without any further approximations or splitting errors. Additional details on the numerical method were reported by Rosenfeld and Israeli[22] for the two-dimensional case and by Rosenfeld et al.[23] for the three-dimensional case.

A typical grid consisted of 15,000–20,000 points: 25 in the normal and circumferential direction and 25–33 points along the spheroid. Full convergence was obtained in 10–20 iterative sweeps. About 1–2 hr of CPU time were needed for a solution on an IBM 3081D computer, depending on the number of grid points and the angle of attack. No standard convergence tests could be performed by systematically increasing the number of grid points because of the excessive computational cost. Nevertheless, some partial accuracy tests were conducted by varying the location of the outer and downstream boundaries while keeping the total number of mesh points constant[23]. No significant differences were recorded for the cases reported in this paper.

Results

The laminar flowfield was solved about two slender prolate spheroids of major to minor axes ratios of 4:1 and 6:1 and for several angles of attack. For the sake of brevity, the results of only two cases will be reported here, one for each axes ratio. The Reynolds numbers chosen are such that laminar flow may be expected to prevail over most of the flowfield (except at separated zones). The streamwise coordinate Z is the normalized axial distance along the spheroid (see Fig. 1) where $Z=-1$ and $Z=1$ correspond to the nose and rear ends of the spheroid, respectively, and $\theta=0$ and 180 deg correspond to the windward and leeward symmetry planes, respectively.

A 4:1 Spheroid at 6-deg Incidence

Several numerical solutions of this case using the boundary-layer equations are reported in the literature.[11-15, 18] No satisfactory experimental results are available for comparison with the numerical calculations. Yet comparison with previous boundary-layer solutions is useful because at such a low incidence the extent of the separated regions is very limited, and therefore, the boundary-layer solutions may be expected to be quite similar to the parabolized Navier-Stokes results over a significant part of the spheroid. The Reynolds number based on half the length of the major axis of the spheroid and on the uniform velocity upstream of the body was set to 10^6. The upstream and downstream boundaries were placed at $Z=-0.8$ and $Z=0.8$, respectively. The upstream conditions were approximated from the boundary-layer solution of Wang.[11]

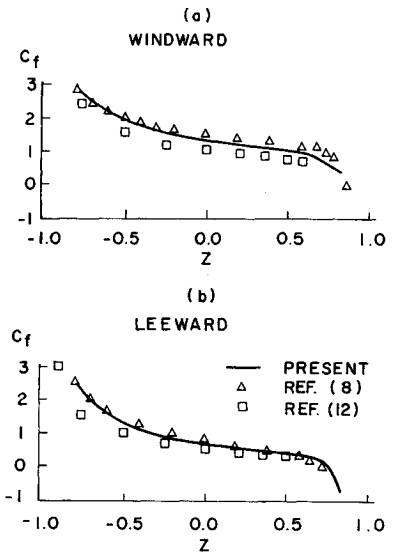

Fig. 2 The distribution of the normalized skin-friction coefficient on the symmetry planes of the 4:1 spheroid at 6-deg incidence.

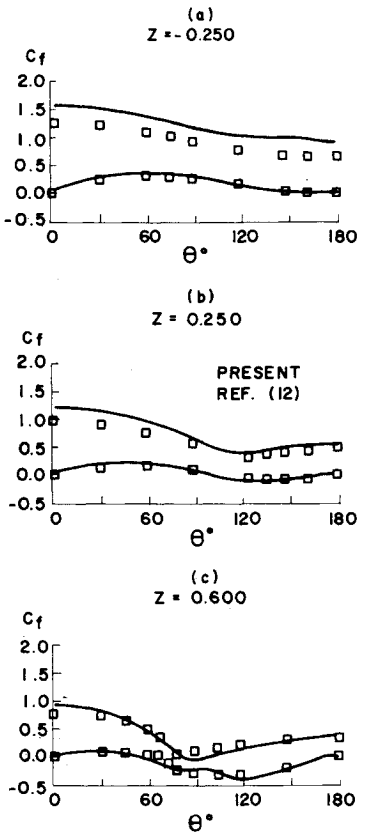

Fig. 3 Comparison of the skin-friction components with the results of Patel and Choi[15] for the 4:1 spheroid at 6-deg incidence.

The distributions of the skin-friction coefficients are compared to the boundary-layer equation results of Wang[11] and Patel and Choi[15] in Figs. 2 and 3. The skin friction is defined as

$$C_F = \frac{\tau_w}{\frac{1}{2}\rho U^2}\sqrt{Re} \tag{7}$$

where Re is the Reynolds number, τ_w is the shear stress on the wall, ρ is the density, and U is the freestream velocity.

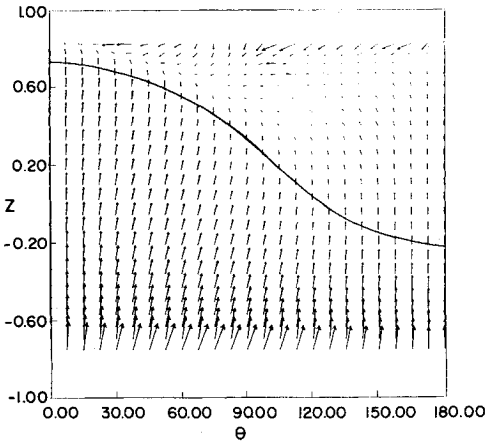

Fig. 4 Skin-friction vector plot for the unwrapped 4:1 spheroid at 6-deg incidence.

Figures 2a and 2b show the distributions of the skin-friction coefficient on the windward and leeward symmetry planes, respectively. Examination of the results shows that the two boundary-layer solutions are not identical. The difference between the two solutions in both the windward side and the upstream part of the leeward side is fairly uniform. Our results generally lie between the two boundary-layer solutions, although we used Wang's solution as the upstream boundary condition. However, in the downstream part of the leeward side, the two boundary-layer solutions approach one another, whereas the present value of the skin friction is somewhat higher. This region is characterized by the thickening of the boundary layer and its ultimate separation. The interaction between the separated flow and the pressure field is expected to lead to quite substantial departures from the potential pressure field specified for the boundary-layer calculations, and consequently, the disagreement between the present and the boundary-layer results might have been expected.

In the present work, separation in the leeward plane starts at $Z=0.75$ (see Fig. 2b). The corresponding singular points computed by the boundary-layer approximation are quite close to one another: $Z=0.724$, $Z=0.72$, and $Z=0.73$ for Wang,[11] Cebeci et al.,[13] and Patel and Choi,[15] respectively. The difference between the boundary-layer results and the present one may be attributed to the viscous-inviscid interaction, which is neglected in the boundary-layer approximation.

The circumferential distribution of the mainstream and the circumferential components of the skin-friction coefficient ($C_{F,\zeta}$ and $C_{F,\theta}$) are shown in Fig. 3 at three axial locations and compared with the data of Patel and Choi.[15] The agreement of the present skin-friction coefficient on the planes of symmetry with Patel and Choi's results is not very good (see Fig. 2), so it is not surprising that the present axial component of the skin friction in the upstream parts of the spheroid differs from the boundary-layer one by a fairly uniform value. Another source of the disagreement can be found in the coarse circumferential resolution used by Patel and Choi: intervals of 20 deg in contrast to 7.5 deg in the present calculation. Still, the circumferential component of the skin friction is in good agreement. The situation is different in the rear part of the spheroid, where the skin-friction lines suggest a circumferentially reversed flow.

The distribution of the calculated skin-friction coefficient vectors on the surface of the spheroid is shown in Fig. 4. The horizontal axis is in the circumferential direction, whereas the vertical axis is in the axial direction. Near the spheroid surface, three different flow regions can be observed. Near the upstream and windward boundaries, the vectors point toward the back and leeward sides of the spheroid. Further downstream and on the leeward side, the directions of the

vectors are shifted in the windward direction, suggesting the onset of a circumferential reversed flow. At the very end of the spheroid, the vectors point toward the nose, indicating the formation of a separation with reverse velocity in the axial direction. The solid line marks the location where the circumferential components of the shear stress reverses its direction—the zero circumferential shear stress line.

The skin-friction lines are tangent to the shear stress vector on the surface and can be computed from[1]

$$\frac{h_s \mathrm{d}s}{h_t \mathrm{d}t} = \frac{C_{F,s}}{C_{F,t}} \tag{8}$$

In steady flows, the skin-friction lines are the projections of the limiting streamlines near the body.[1] Therefore, their pattern may be instructive of the flowfield in the vicinity of the body. Lighthill[3] has shown that in the three-dimensional case, flow separation from a solid body may be connected with either vanishing skin friction $|C_F| \to 0$ (at singular points) and/or the convergence of the skin-friction lines into one particular line.

In the present work, the skin-friction lines were computed by solving Eq. (8) with a second-order Runge-Kutta method. The components of the skin friction are interpolated using a bilinear spline approximation. The skin-friction lines for the 4:1 spheroid at 6-deg incidence are shown in Figs. 5. Figure 5a shows the pattern on the coordinate plane Z-θ, while the side, bottom, and upper views of the skin-friction lines on the spheroid are shown in Fig. 5b. Two types of skin friction lines convergence are evident: a very short swept line and a second line that appears to encircle the spheroid at about $Z = 0.70$. The second line of convergence is obviously a separation line that passes through singular points and divides the flow into two regions: a region that is accessible to the flow from the forward stagnation point and a region that is not accessible. Figure 6 compares the zero circumferential shear stress line and the closed separation line with the boundary-layer results of Wang[12] and Cebeci et al.[13] The qualitative shape of the closed separation line is similar to these computations although the "tongue" of the separation line in our results is less pronounced and closer to the windward side. The agreement of the zero circumferential shear stress line is much better, indicating that the boundary-layer approximation is valid in regions far from a flow separation. Although there is circumferential flow reversal from about $Z = -0.1$, the skin-friction lines converge only at $Z = 0.45$, and about 15 deg further in the leeward direction to the zero circumferential shear stress line (see Fig. 5a). However, the pattern of the skin-friction lines is not sufficient to conclude whether a vortex-type separation has occured. The definite identification of a flow separation should be based on the analysis of the whole flowfield.[7,8]

The topology of the skin-friction lines found in our calculations is notably similar to that conceived by Han and Patel[6] from their flowfield visualizations of the flow over a 4.3:1 spheroid at 10-deg incidence and a Reynolds number of 4.10^4 (see Fig. 10 in Han and Patel[6]). Although neither shown nor computed, two nodes of attachment exist at the upstream and downstream stagnation points. The pattern of the skin-friction lines reveals the existence of a saddle point at the rear part of the leeward symmetry plane, with two separatrixes[9] (separation lines that emanate from the saddle point) encircling the body. The short swept convergence line bends into the separatrix. Cebeci et al.[13] suggest three possibilities for the shape of the swept convergence line near the closed convergence line. The present results seem to confirm their second option (Fig. 10 in Cebeci et al.[13]). The point where the two convergence lines blend together is necessarily a node-type singular point. Because another node exists at the other side of the spheroid, an additional saddle point should exist to satisfy the topological rule stated by Lighthill.[3] This saddle point is at the windward symmetry

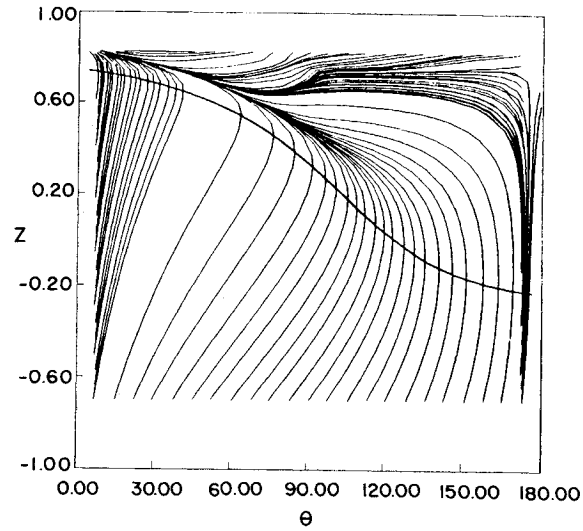

Fig. 5a Skin-friction lines on the unwrapped 4:1 spheroid at 6-deg incidence.

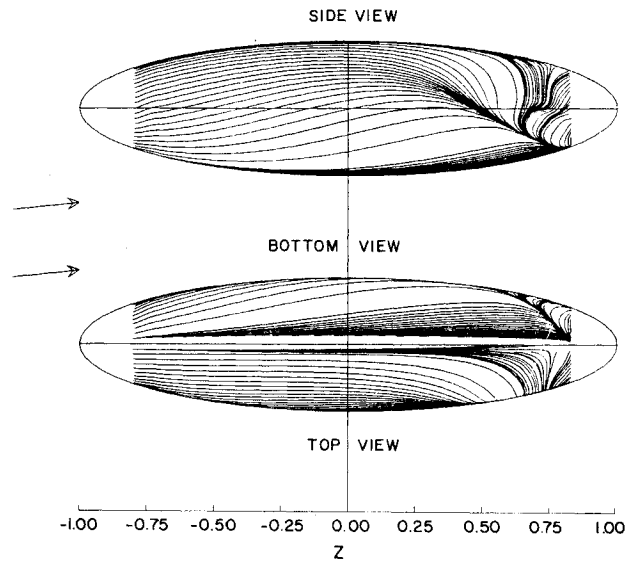

Fig. 5b Skin-friction lines on the 4:1 spheroid at 6-deg incidence.

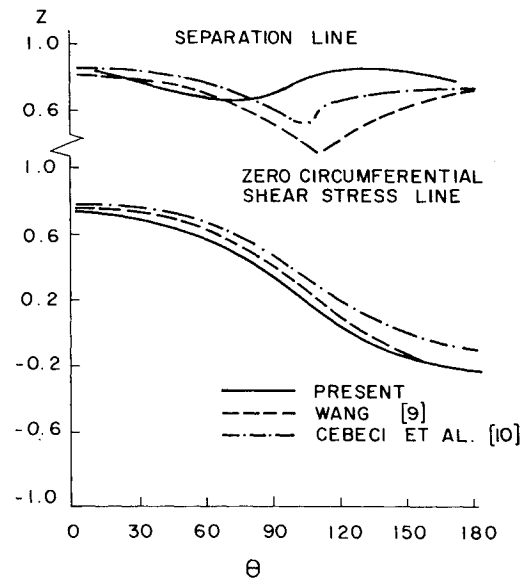

Fig. 6 Comparisons of the separation and of the zero circumferential shear stress lines with other results for the 4:1 spheroid at 6-deg incidence.

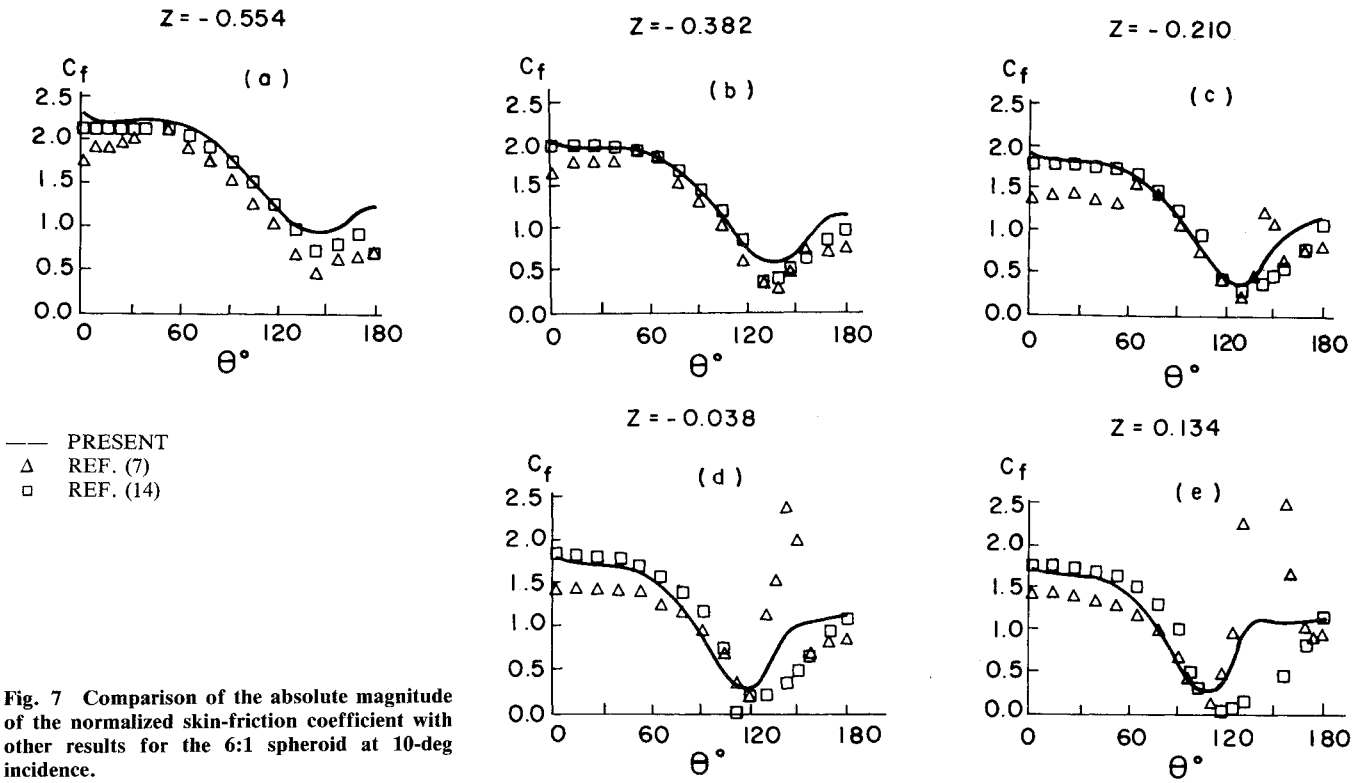

Fig. 7 Comparison of the absolute magnitude of the normalized skin-friction coefficient with other results for the 6:1 spheroid at 10-deg incidence.

plane. However, it is not discovered in the present calculation because the it is located outside the domain of solution.

A 6:1 Spheroid at 10-deg Incidence

In this higher-incidence case, the separated flowfield has a more complicated form. Some boundary-layer solutions were reported for this case,[16-19] as well as a thin-layer computation.[20] The experimental data available are reported by Kreplin et al.,[10] who measured the shear stress on a 6:1 spheroid at a Reynolds number of 8.10^5 (based on half of the main axis). The same Reynolds number was used in the present calculations. The upstream and downstream boundaries were located at $Z=-0.9$ and $Z=0.7$, respectively.

The absolute magnitude of the shear stress in several axial stations is compared in Fig. 7 with experimental values[10] and with the computed boundary-layer results of Patel and Baek.[17] The agreement at small distances from the upstream boundary is not good, possibly due to poor specification of the upstream boundary conditions in the present calculations (they were approximated from Stock's integral boundary-layer solution[18]). Further downstream, the agreement of our calculation with the experimental results improves, while the results of Han and Baek get worse. The poor agreement with experiments on the leeward side is probably related to the transition of the separated flow to turbulent flow, as noted by Kreplin et al.[10] In our laminar calculation, this phenomenon cannot be reproduced.

Figure 8 shows the shear stress vector plot on the spheroid. The existence of a minimum in the shear stress along the circumferential direction is clearly seen. It is interesting to note that due to three-dimensional effects, this minimum does not occur along the leeward side, where the potential circumferential adverse pressure gradient is maximal. Figure 9a shows a comparison of the shear stress vector plot interpolated from our computations with the experimental results of Kreplin et al.[10] In the laminar region of the flowfield, the agreement is usually good, bearing in mind the complexity of the flowfield and the difficulties in measuring the stress in the laminar regions, as reported by Kreplin et al. However, the agreement at the upstream stations near the leeward side is not as good. This is attributed

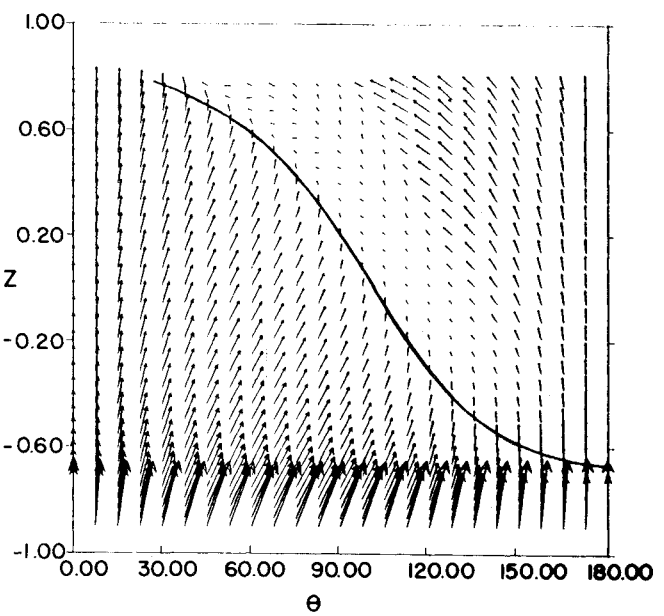

Fig. 8 Skin-friction vector plot for the unwrapped 6:1 spheroid at 10-deg incidence.

to the poor upstream boundary conditions used in the present calculation at the upstream boundary. Figure 9b shows the same comparison with the high-accuracy boundary-layer results of Schoenauer.[16] A boundary-layer solution was not obtained for significant parts of the flowfield, although these are the most interesting regions in which separation may occur. In the other regions, agreement with our results is even better than with the experimental results.

Figure 10 shows the skin-friction lines on the surface. In the present domain of solution, neither singular points nor a closed separation line is found. However, a long and swept convergence line is present, with skin-friction lines merging into it from both sides. The precise origin of the convergence line cannot be defined with certainty, and no singular points

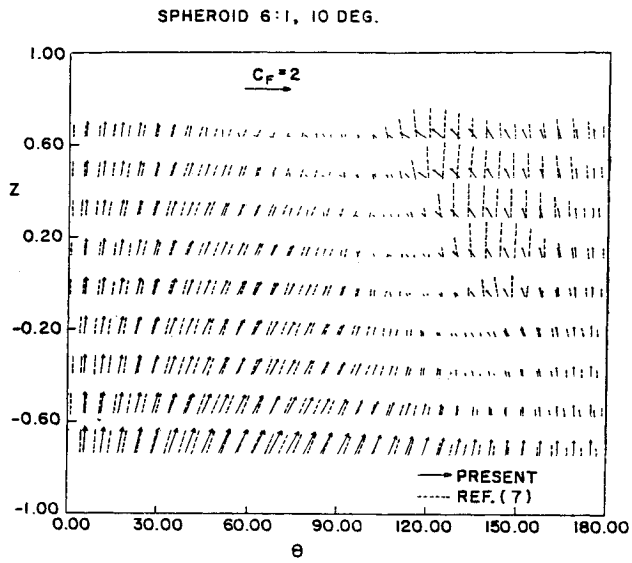

Fig. 9a Computed skin-friction coefficient compared to Kreplin et al.[10] experiments.

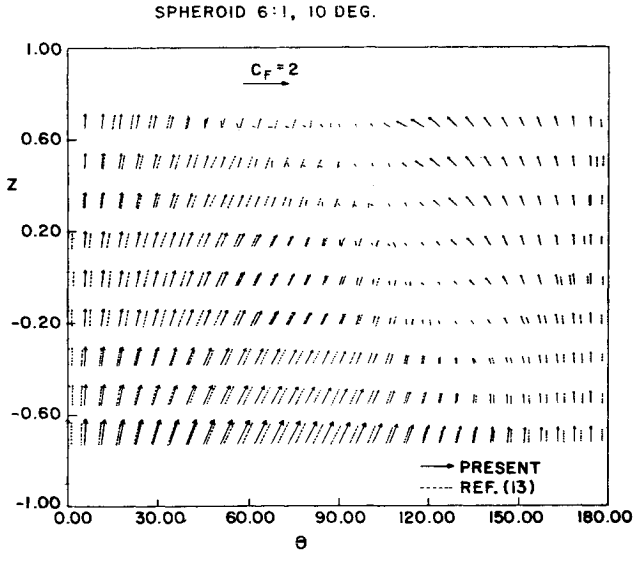

Fig. 9b Computed skin-friction coefficient compared to boundary-layer results of Schoenauer.[16]

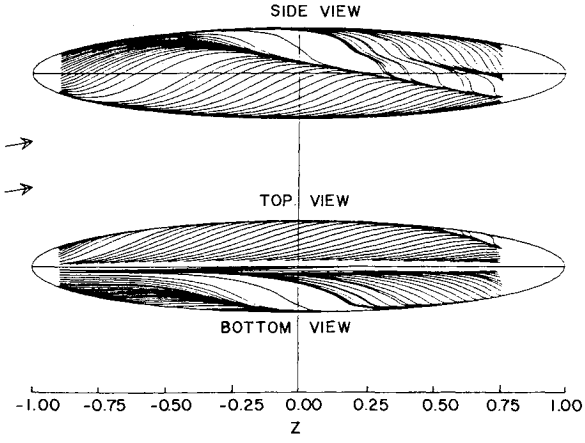

Fig. 10a Skin-friction lines on the unwrapped 6:1 spheroid at 10-deg incidence.

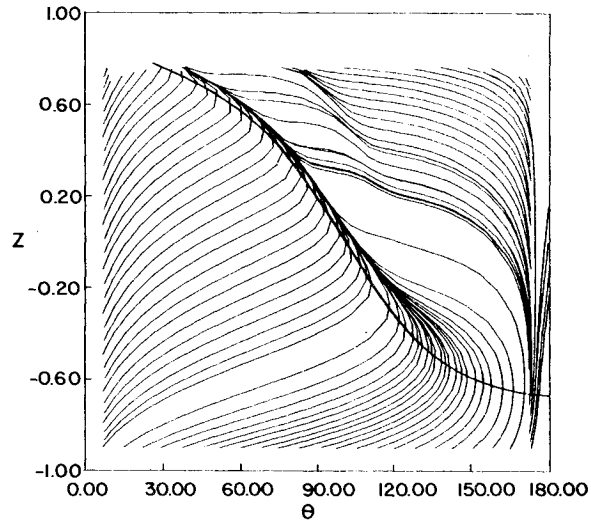

Fig. 10b Skin-friction lines on the 6:1 spheroid at 10-deg incidence.

can be detected on the upstream part of the swept convergence line, at least with the present resolution of the computation. Now the zero circumferential shear stress line is only a small distance in the windward direction from the convergence line. Again, it is impossible to predict the location of the onset of a separation based on the properties of the flowfield in the vicinity of the surface. Numerous results[6,17,19,20] as well as further study by the present authors (not detailed here) suggest that a vortex-type[1,5] separation exists in this case.

Kreplin et al. obtained the skin-friction lines from the measured distribution of the shear stresses (Fig. 5 in Ref. 10). The main separation line appears to be placed further in the leeward direction than the line we have computed. The differences may be explained by the transition to turbulent flow that occurred in the experiment because turbulent flow can withstand higher adverse circumferential pressure drop before separation. Kreplin et al.[10] observed a second separation line very close to the leeward side. We have not found this line, although there is a tendency to create a second convergence line in the rear part of the spheroid. Pan and Pulliam,[20] who used the thin-layer equations, obtained better agreement in the laminar case with the experimental skin-friction lines of Kreplin et al., although the separation in the real flow is turbulent.

Conclusions

The incompressible, steady, and laminar parabolized Navier-Stokes equations were used to simulate the flowfield around a prolate spheroid. Solutions were obtained in the entire flowfield, including regions of attached flow as well as regions of separated flow. The computer resources required for the calculations were not prohibitive, although such calculations would be better performed on a supercomputer.

In the parabolized Navier-Stokes approximation, as used in the present work, all the equations (the continuity plus the three momentum equations) should be solved for the full set of primitive variables (the pressure plus the three velocity components). Consequently, it may be expected that the approximation will be superior to the parabolic boundary-layer approximation. This is fully supported by the present results, which did not show any abnormal or singular behavior of the solution near separation lines, as is found in boundary-layer solutions. Indeed, the method was capable of yielding solutions in all flow regions, demonstrating that the parabolized approach is a suitable candidate for the calculation of three-dimensional viscous flowfields on slender bodies.

In the present paper, we report the distribution of the skin friction on the surface of the spheroid only. Even with this

limitation, the information is useful because it shows some features of the flowfield and allows comparisons with available experimental and numerical data. It should be remembered that most of the available data are confined to the skin friction anyhow. Comparison of the results with previous experimental data and numerical solutions of the boundary-layer approximation reveals good agreement in the attached-flow regions. However, in the separated flow region the calculated skin friction is too low compared to the experimental data, presumably due to transition to turbulent flow. The zero circumferential skin-friction line lies windward of the line to which the skin-friction lines converge. The distance between them decreases as the incidence increases. As no unique relationship exists between the skin-friction lines and the flowfield, it is impossible to draw any conclusions from the results shown on the structure of three-dimensional flow separation.

Finally, some conclusions on the need for future work are in order. It is necessary to perform a turbulent calculation in order to cater to the turbulent regions near and downstream of separation. The analysis must be extended to the entire flowfield. Such a study requires the use of supercomputers for the computations and graphic workstations for analyzing, visualizing, and understanding the results.

Acknowledgment

The research was partially supported by Stiftung Volkswagenwerk Grant 1/37270.

References

[1]Peake, D. J. and Tobak, M., "Three-Dimensional Interactions and Vortical Flow with Emphasis on High Speeds," AGARDograph 252, July 1980.

[2]Maltby, R. L., "Flow Visualization in Wind Tunnels Using Indicators," AGARDograph 70, 1962.

[3]Lighthill, M. J., "Attachment and Separation in Three-Dimensional Flow in Laminar Boundary Layers," *Laminar Boundary Layers*, Oxford University Press, London, 1963, pp. 72–82.

[4]Maskell, E. C., "Flow Separation in Three-Dimensions," RAE Aeronautics Report 2565, 1955.

[5]Wang, K. C., "Separation Patterns of Boundary Layer Over an Inclined Body of Revolution," *AIAA Journal*, Vol. 10, Aug. 1972, pp. 1044–1050.

[6]Han, T. Y. and Patel, V. C., "Flow Separation on a Spheroid at Incidence," *Journal of Fluid Mechanics*, Vol. 92, 1979, pp. 643–657.

[7]Dallmann, U., "Topological Structures of Three-Dimensional Vortex Flow Separation," AIAA Paper 83-1735, 1983.

[8]Wang, K. C., "On the Disputes About Open Separation," AIAA Paper 83-0296, 1983.

[9]Chapman, G. T., "Topological Classification of Flow Separation on Three-Dimensional Bodies," AIAA Paper 86-0485, 1986.

[10]Kreplin, H. P., Vollmers, H., and Meier, H. U., "Measurements of the Wall Shear Stress on an Inclined Prolate Spheroid," *Zeitschrift fur Flugwissenschaft Weltraumforschung*, Vol. 6, 1982, pp. 248–252.

[11]Wang, K. C., "Three-Dimensional Boundary Layer Near the Plane of Symmetry of a Spheroid at Incidence," *Journal of Fluid Mechanics*, Vol. 43, 1970, pp. 187–209.

[12]Wang, K. C., "Boundary Layer Over a Blunt Body at Low Incidence with Circumferential Reversed Flow," *Journal of Fluid Mechanics*, Vol. 72, 1975, pp. 49–65.

[13]Cebeci, T., Khattab, A. A., and Stewartson, K., "Three-Dimensional Laminar Boundary Layers and the Ok of Accessibility," *Journal of Fluid Mechanics*, Vol. 107, 1981, pp. 57–87.

[14]Hirsch, R. S. and Cebeci, T., "Calculation of Three-Dimensional Boundary Layers with Negative Cross Flow on Bodies of Revolution," AIAA Paper 77-683, 1977.

[15]Patel, V. C. and Choi, D. H., "Calculation of Three-Dimensional Laminar and Turbulent Boundary Layers on Bodies of Revolution at Incidence," *Turbulent Shear Flows II*, edited by L. J. S. Bradbury, F. Durst, B. E. Launder, F. W. Schmidt, and J. H. Whitelaw, Springer-Verlag, New York, 1980, pp. 199–217.

[16]Schoenauer, W., private communication, 1984.

[17]Patel, V. C. and Baek, J. H., "Boundary Layers and Separation on a Spheroid at Incidence," *AIAA Journal*, Vol. 23, Jan. 1985, pp. 55–63.

[18]Stock, H. W., "Laminar Boundary Layers on Inclined Ellipsoids of Revolution," *Zeitschrift fur Flugwissenschaft Weltraumforschung*, Vol. 4, 1980, pp. 217–224.

[19]Van Dalsem, W. R. and Steger, J. L., "The Efficient Simulation of Separated Three-Dimensional Viscous Flows Using the Boundary Layer Equations," AIAA Paper 85-4064, 1985.

[20]Pan, D. and Pulliam, T. H., "The Computation of Steady 3-D Separated Flows Over Aerodynamic Bodies at Incidence and Yaw," AIAA Paper 86-0109, 1986.

[21]Haase, W., "Separation and Vortex Pattern on a Spheroid at Incidence." *Proceedings of 5th USAF/FRG Data Exchange Agreement Meeting*, AFFDL-TR-80-3088, 1980, pp. 287–305.

[22]Rosenfeld, M. and Israeli, M., "Numerical Solution of Incompressible Flows by a Marching Multi-Grid Nonlinear Method," *AIAA Journal*, Vol. 25, May 1987, pp. 641–647.

[23]Rosenfeld, M., Israeli, M., and Wolfshtein, M., "A Numerical Method for the Solution of Three Dimensional, Incompressible, Viscous Flows Over Slender Bodies," *Numerical Methods in Laminar and Turbulent Flow*, edited by C. Taylor, W. G. Habashi, and M. M. Hafez, Pineridge Press, Swansea, 1987, pp. 2014–2028.